Journal of Catalysis **182,** 441–448 (1999)
Article ID jcat.1998.2334, available online at http://www.idealibrary.com on IDEAL®

A Model of Oxygen Transport in Pt/Ceria Catalysts from Isotope Exchange

Anna Holmgren,* Daniel Duprez,† and Bengt Andersson*,[1]

*Department of Chemical Reaction Engineering, Chalmers University of Technology, SE-412 96 Göteborg, Sweden; and †Laboratoire de Catalyse en Chimie Organique, 40 Avenue de Recteur Pineau, 86022 Poitiers Cedex, France

Received July 30, 1998; revised October 28, 1998; accepted November 3, 1998

From isotope oxygen exchange reactions and simulations of these experiments, the important steps in oxygen transport in Pt/ceria were distinguished and their rates were estimated. A Pt/alumina sample was also experimentally investigated for comparison. Oxygen surface diffusion as well as oxygen spillover from Pt to ceria was found to be fast in comparison with adsorption/desorption of oxygen on the metal and oxygen bulk diffusion. The exchange rate was found to be higher on a very-low-Pt-dispersion sample than on a high-dispersion sample, which in the model was explained by the different adsorption properties of oxygen.

Key Words: **ceria; platinum; oxygen transport; oxygen exchange; mathematical modeling.**

INTRODUCTION

Use of an oxygen storage component in the catalysts that clean car exhaust was proposed by Ghandi *et al.* in 1976 (1), and was generally implemented in the catalysts in the beginning of the 1980s. The major role of the oxygen storage component, usually a base metal oxide, is to act as an oxygen buffer, compensating for the deviations from stoichiometry in the exhaust gas. Cerium oxide is one of the most frequently used oxygen-storing components in car exhaust catalysts (2). In recent years, it has generally been replaced by a solid solution of CeO_2–ZrO_2, due to the improved thermal stability (3, 4), reducibility (5), and oxygen transport (6) of this system. Other dopants, with lower valence than Zr, have also been tested (7–9). These dopants provide the advantage of increasing the number of oxygen vacancies, which causes oxygen mobility to increase.

Oxygen isotope exchange is a common method used to study the adsorption/desorption properties of oxygen and the participation of oxygen from the catalyst in oxidation reactions (10). Steele and Floyd (11) measured the oxygen diffusion rate through ceria by performing oxygen isotope exchange at 850–1100°C. They observed a strong dependence of the diffusion rate on the concentration of oxygen vacancies, and concluded that the diffusion occurs via a vacancy mechanism. Martin and Duprez estimated the surface and bulk diffusion coefficients at 350–400°C by performing oxygen isotope exchange on various Rh-impregnated supports (12). In their study, the coefficients of surface diffusion were determined by using the model of circular sources developed by Kramer and Andre (13). For bulk diffusion, Martin and Duprez used a method described by Kakioka *et al.* (14), in which the gas and the surface are assumed to be in equilibrium, having the same isotope ratio. Klier and Kucera (15) solved analytically the problem of first-order isotope exchange at the surface and diffusion in the bulk for spherical, cylindrical, and planar geometries. In the present work, we adopted a similar approach as the one used in the work of Martin and Duprez (12), by performing temperature-programmed isotope exchange (TPIE). However, we have done more extensive modeling, including the adsorption and desorption steps on the metal, the spillover from metal to support, the direct exchange between the gas and the ceria surface, and the oxygen diffusion in the ceria bulk. By this procedure, the rate-determining steps in the oxygen storage could be determined, and the kinetic parameters of these steps were estimated. Besides Pt/ceria and ceria, a Pt/alumina catalyst was also investigated for comparison.

EXPERIMENTAL METHODS

Catalyst Samples

Ceria, Pt/ceria, and Pt/alumina powder catalysts were used. The properties of the catalyst samples are shown in Table 1. The ceria support was prepared by calcining cerium oxide from Rhône–Poulenc (cerium oxide 99.5 H.S.A. 514) in air for 2–4 h at 900°C. The ceria was impregnated with a solution of H_2PtCl_6, freeze-dried overnight, and then calcined for 2 h at 550 or 900°C. The variation in calcination temperature resulted in one high-Pt-dispersion (HD) sample and one low-Pt-dispersion (LD) sample. These two samples are considered to be representative of a fresh sample

[1] To whom correspondence should be addressed. Fax: +46–31–772 30 35. E-mail: bengt@cre.chalmers.se.

0021-9517/99 $30.00

TABLE 1

Catalyst Properties

Catalyst	Treatment	Pt dispersion	Surface Pt (μmol/g catalyst)	BET (m^2/g)
Ceria	Calc. 900°C 4 h	—	—	71
3% Pt(HD)/ ceria	Ceria calc. 900°C 2 h, Pt/ceria calc. 550°C 2 h	0.09[a]	14	53
3% Pt(LD)/ ceria	Ceria calc. 900°C 2 h Pt/ceria calc. 900°C 2 h	0.004[a]	1	39
2.5% Pt/ alumina	Calc. 500°C 2 h	0.24[b]	28	151

[a] From TEM images.
[b] From CO chemisorption at 25°C, assuming an adsorption stoichiometry of 1 : 1.

and a severely aged sample. On the LD sample, the Pt particle size is much larger than the average ceria crystal size, and it is more relevant to talk about a Pt–CeO_2 mixture rather than a supported catalyst. The Pt dispersion on these samples was estimated from TEM (CM 120 Philips) images. The samples were crushed, ultrasonically suspended in ethanol, and then deposited on a Cu grid previously covered with a thin layer of carbon. The Pt dispersion was calculated from the observed Pt particle sizes, with the assumption that the Pt particles were half-spherical. This microscopic determination of the Pt dispersion was used instead of the standard CO or H_2 chemisorption method due to the large CO and H_2 adsorption capacity of ceria itself, in particular in the presence of noble metals (16–18). The Pt/alumina sample was prepared by impregnating γ-Al_2O_3 with H_2PtCl_6 and then calcining for 2 h at 500°C. The Pt dispersion was on this sample estimated by CO chemisorption at 25°C.

Measurements of Oxygen Exchange

Oxygen isotope exchange experiments were conducted in a gas recirculation reactor system, equipped with a tubular quartz reactor, a pump (Metal Bellows MB-41E) to recirculate gas, and a vacuum pump to evacuate the system. A mass spectrometer (QMG 420 Balzers) was used to continuously sample gas. The reactor setup is shown in Fig. 1. The temperature-programmed isotope oxygen exchange between the ^{16}O of the catalyst and $^{18}O_2$ from the gas phase was studied in the temperature interval 25–600°C. The sample weight was adjusted so that each sample would have a total BET surface area of 2.5 m^2, since it is assumed that the exchange is a surface-initiated process. The pretreatment comprised oxidation in flowing $^{16}O_2$ at 400°C for 15 min, evacuation at 400°C for 15 min, reduction in flowing H_2 at 400°C for 15 min, evacuation at 400°C for 30 min, and cooling to 25°C *in vacuo*. The samples were then exposed to 50 mbar of $^{18}O_2$ (98.6% purity, Isotec) at 25°C, and the temperature of the sample was raised to 600°C with a ramp speed of 2°C/min. The gas was continuously recirculated through the catalyst bed with a high flow rate (nominal recirculation rate: 180 cm^3/s at reactors P and T), so that differential conditions would prevail in the bed. The masses 32, 34, and 36 were recorded in the mass spectrometer every 10 s. In addition, mass 18 was recorded to detect water formation due to desorption of hydroxyl groups or due to oxidation of residual hydrogen. To detect possible leaks, mass 28 was also recorded. The reproducibility of the temperature-programmed oxygen exchange had earlier been investigated on a ceria and a Rh/ceria sample, for which four repeated experiments were conducted (19). The resulting curves could be superimposed with a maximum temperature difference of 5°C, which showed that the reproducibility is satisfying.

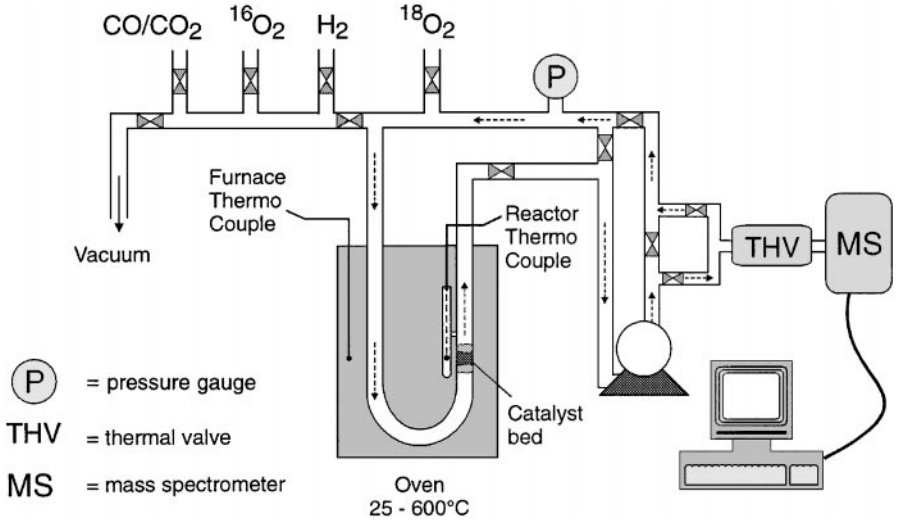

FIG. 1. Experimental setup in the exchange experiments.

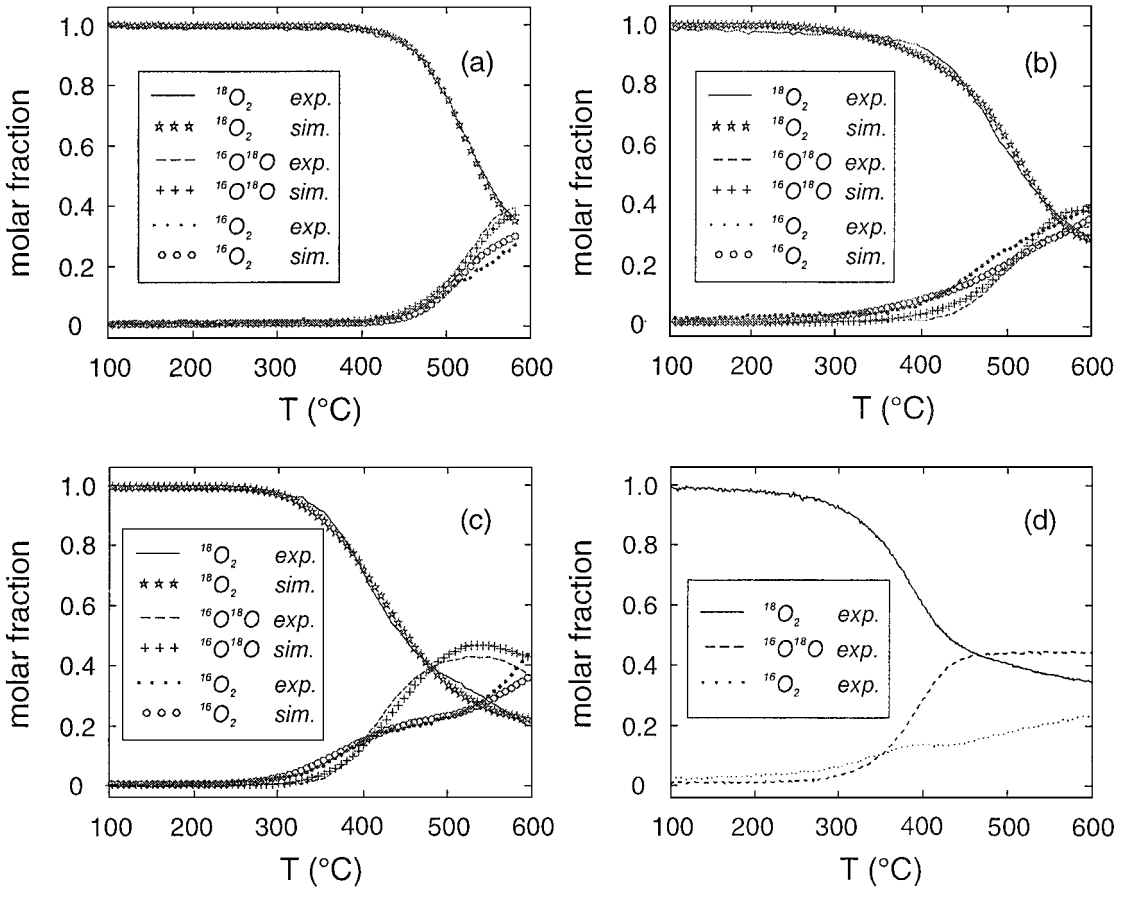

FIG. 2. Experimental and simulated results of oxygen exchange on (a) ceria, (b) 3% Pt(HD)/ceria, and (c) 3% Pt(LD)/ceria and (d) experimental results for 2.5% Pt/alumina.

RESULTS AND DISCUSSION

Oxygen Exchange

Figure 2 shows the changes in the gas phase concentrations of the oxygen isotopes between 100 and 600°C. Below 100°C there was little or no exchange. Modeling results are also given, and are discussed in a following section. The exchange is seen to start at about 450°C on ceria, at 400°C on 3% Pt(HD)/ceria, at 350°C on the sintered 3% Pt(LD)/ceria, and at about 300°C on 2.5% Pt/alumina. This means that the sample with the highest oxygen storage capacity [measured in a CO/O_2 pulse experiment (20)] is the least active in oxygen exchange, and vice versa. This may seem surprising since many of the steps in these two processes are the same, e.g. adsorption, diffusion, and removal/insertion of oxygen. However, an important difference is that during oxygen exchange, oxygen has to desorb to create a new site for oxygen to adsorb, whereas during OSC, these sites are created by the reducing agent. Moreover, it requires less energy to replace oxygen than to remove it, which means that oxygen that cannot be reduced can participate in oxygen exchange. The results emphasize that oxygen desorption is rate limiting during the exchange, and that this occurs more easily from the alumina-supported Pt than from the ceria-supported Pt.

The amount of exchanged oxygen is shown in Fig. 3. It is calculated from the mass balance of ^{18}O. Since the

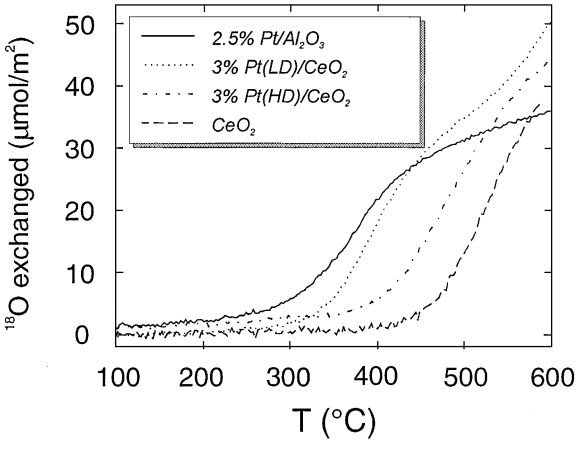

FIG. 3. Amount of oxygen exchanged into the catalyst as a function of temperature.

experiments were conducted in a closed reactor system, all ^{18}O must be either in the gas, on the surface of the metal or the support, or in the bulk of the support. The fraction of ^{18}O in the gas, α_g, is easily obtained from the molar fractions of the isotopes:

$$\alpha_g = 0.5y_{34} + y_{36}. \quad [1]$$

The amount of oxygen that has been exchanged into the catalyst is then calculated from

$$O_{\text{exchanged}} = 2(1-\alpha_g)\frac{pV}{RTA_{\text{catalyst}}}. \quad [2]$$

As seen from Fig. 3, Pt/alumina is the most efficient catalyst for oxygen exchange below 400°C. Surprisingly, large amounts are exchanged. Already at 400°C, 20 μmol/m^2 has been exchanged. Since the saturation amount of OH groups on alumina is 10 μmol/m^2 (21) [the OH group density after reduction in hydrogen at 400°C is lower, probably around 5 μmol/m^2 (22)], this means that there is also exchange with oxygen in the Al_2O_3 lattice. In Fig. 3 it is also seen that the LD Pt/ceria is more efficient than the HD Pt/ceria in the oxygen exchange. The HD Pt/ceria is not significantly better than ceria without Pt, which is consistent with earlier observations (23).

For the ceria catalysts, there is evolution of both $^{16}O_2$ and $^{18}O^{16}O$, in contrast to the results of Cunningham *et al.* (24), who observed only $^{16}O_2$ and no $^{18}O^{16}O$ in the temperature range 450–650°C. The total amount of oxygen that is exchanged corresponds to about 25% of all oxygen in the ceria lattice being exchanged to ^{18}O, neglecting that there is likely also exchange with OH groups on ceria. The OH group density on ceria was estimated by H/D exchange by Martin and Duprez (22). After reduction in hydrogen at 450°C, there was about 4.6 μmol OH/m^2. After evacuation at 450°C, similar to our treatment, this value was reduced by about a factor of 2. This means that, on CeO_2, the exchange with OH groups is small in comparison with the exchange with lattice oxygen. The total amount of surface oxygen (OH groups and lattice oxygen at the surface) is about 25 μmol/m^2, which means that bulk oxygen must be exchanged above 400–550°C.

When the ceria-containing catalysts were exposed to $^{18}O_2$ at 25°C, oxygen was consumed in their reoxidation, which is known to occur easily at room temperature (25). Possibly, there was additional oxidation in the temperature interval 25–600°C. The amount could not be determined from the observed pressure decrease during the exchange though, since small amounts of gas were continuously removed to the MS. Moreover, there were probably small leaks of atmosphere into the reactor, since mass 28 (nitrogen) showed a slow, continuous increase during the exchange. If the corresponding amount of oxygen leaked in, this would correspond to an additional $^{16}O_2$ molar fraction of up to 0.06. This was found negligible and has not been corrected for, but may explain the slow, linear increase in $^{16}O_2$ at temperatures below 300–400°C for 2.5% Pt/alumina, 3% Pt(HD)/ceria, and 3% Pt(LD)/ceria.

Modeling Oxygen Exchange on Ceria and Pt/Ceria

The Pt/alumina sample was left out from the modeling since a quantification of the oxygen transport properties in this sample is of minor interest due to the poor oxygen storage capacity of alumina. For the ceria and Pt/ceria samples, the following three observations from the exchange experiments helped us develop a model:

1. On ceria, the initial rates of $^{16}O^{18}O$ and $^{16}O_2$ formation were about equal (see Fig. 2a). This indicates that there is both single and multiple heteroexchange (26) on ceria, as earlier observed (12). The single heteroexchange was modeled according to Winter (27),

$$^{18}O_{2(g)} + {}^{16}O_{(s)} \underset{r_{-1}}{\overset{r_1}{\rightleftarrows}} {}^{18}O^{16}O_{(g)} + {}^{18}O_{(s)} \quad [3]$$

with

$$r_1 = k_{\text{exch.single}}\, p_{^{18}O_2}\theta_{^{16}O}, \quad [4]$$

$$r_{-1} = \frac{k_{\text{exch.single}}}{2}\, p_{^{18}O^{16}O}\theta_{^{18}O}, \quad [5]$$

and analogously for exchange between $^{16}O_{2(g)}$ and $^{18}O_{(s)}$. The multiple exchange can be written (27)

$$^{18}O_{2(g)} + 2{}^{16}O_{(s)} \underset{r_{-2}}{\overset{r_2}{\rightleftarrows}} {}^{16}O_{2(g)} + 2{}^{18}O_{(s)}, \quad [6]$$

with

$$r_2 = k_{\text{exch.multi.}}\, p_{^{18}O_2}\theta^2_{^{16}O}, \quad [7]$$

$$r_{-2} = k_{\text{exch.multi.}}\, p_{^{16}O_2}\theta^2_{^{18}O}, \quad [8]$$

and with analogous expressions for exchange between either $^{18}O_{2(g)}$ or $^{16}O_{2(g)}$ and one $^{16}O_{(s)}$ plus one $^{18}O_{(s)}$. The surface species responsible for the multiple exchange are assumed to consist of two adjacent O species in a special environment or, maybe, of binuclear species such as peroxide or superoxide anions (28). In reality, the mechanisms of exchange are probably more complicated, including adsorption of gas-phase oxygen, but the above scheme was sufficient to account for the direct exchange on ceria.

2. On Pt/ceria, $^{16}O_2$ formation started at a lower temperature than $^{16}O^{18}O$ formation. This observation was surprising, since Pt is expected to increase the capacity for oxygen dissociation. If $^{18}O_2$ dissociates into two $^{18}O_{ads}$ on a catalyst containing mainly ^{16}O, one expects the formation of $^{16}O^{18}O$. The only way that we could simulate the observed behavior was if the surface was initially covered mainly with ^{16}O. Moreover, there had to be rapid mixing between the adsorbed ^{18}O and the ^{16}O, so that ^{16}O was in large excess

on the surface. Such behavior demands that the following points (a–c) are valid:

a. If there is to be no enrichment of ^{18}O at the surface, a homogeneous distribution of vacancies must be created during the reduction. Alternatively, if the reduction causes a nonhomogeneous distribution, it must be made more homogeneous during the oxidation. There are few data on the bulk oxygen diffusion rate in ceria. Martin and Duprez (12) estimated the oxygen bulk and surface diffusion rates in ceria by oxygen exchange studies on Rh/ceria. They reported an oxygen bulk diffusion coefficient in oxidized ceria at 350°C of 5×10^{-22} m^2/s. If we assume that oxygen has to diffuse half the average particle diameter (the ceria particles are assumed to be spherical), which is about 12 nm for our samples, the time for such a diffusion is approximately $L^2/D_b = 20$ h.[2] This means that the pretreatment of about 45 min (reduction for 15 min and evacuation for 30 min) would not suffice. However, the degree of ceria reduction is very important to the diffusion rate. Steele and Floyd (11) showed that oxygen diffusion at 850–1150°C was 25 times faster for $CeO_{1.92}$ than for CeO_2 at 850°C. If the Steele and Floyd data were to be extrapolated to 400°C (which is questionable, since the mechanism of exchange may be different) the difference would be even larger: the diffusion rate would be 1000 times faster in $CeO_{1.92}$ than in CeO_2 at 400°C. In conclusion, it does not seem unlikely that the reductive pretreatment will create a fairly homogeneous distribution of oxygen vacancies. The isotope composition can be estimated from the decrease in oxygen pressure in the reactor during reoxidation at 25°C, and was, e.g., about $Ce^{16}O_{1.88}{}^{18}O_{0.12}$ for HD Pt/ceria.

b. Oxygen diffusion on the ceria and Pt surfaces is fast compared with adsorption/desorption of oxygen and bulk diffusion, so that a complete mixture of the isotopes is achieved at the surface. Martin and Duprez (12) measured oxygen surface diffusion on ceria. They obtained the value 5.7×10^{-16} m^2/s at 400°C. Thus, surface diffusion was found to be about six orders of magnitude faster than bulk diffusion, so it seems reasonable to assume that surface diffusion is fast. However, for the LD sample, the Pt particles are far apart. The average particle size is 0.3 μm and the average distance between the particles is above 1 μm, the exact value depending on the particle distribution. Still, given the experimental results, we have kept the assumption of fast surface diffusion.

c. Furthermore, for a fast mixture of isotopes on the surface to take place, the spillover of oxygen has to be fast in comparison with the adsorption/desorption of oxygen. This was observed earlier for Pt/ceria (23). In some simulations, a spillover step between Pt and ceria was included. However, it was found that to simulate the behavior in terms of early evolution of $^{16}O_2$, the spillover has to be fast and not rate determining in the exchange.

3. Exchange with the surface oxygen was not sufficient to explain the large quantities of oxygen exchange. Thus, the bulk of the ceria also had to be included. This was done by adding the following mass balance for the fraction of ^{18}O in the ceria bulk, α_b:

$$\frac{\partial \alpha_b}{\partial t} = D_b \frac{1}{r^2}\left(\frac{\partial}{\partial r}\left(r^2 \frac{\partial \alpha_b}{\partial r}\right)\right). \quad [9]$$

Here D_b is the diffusion coefficient in m^2/s. This partial differential equation was solved by orthogonal collocation, using six internal collocation points (29). This results in six initial value problems, one in each collocation point r_i,

$$\frac{d\alpha_b(r_i)}{dt} = D_b \sum_{j=1}^{6} B_{ij}\alpha_b(r_i), \quad i = 1, 2, \ldots, 6, \quad [10]$$

where

$$B = DQ^{-1}, \quad [11]$$

with

$$Q_{ij} = r_i^{2j-2} \quad [12]$$

and

$$D_{ij} = (2j-2)(2i-1)r_i^{2j-4}. \quad [13]$$

Only polynomials of even order were used to approximate α_b. The six initial value problems above were solved coupled with the boundary condition at the ceria surface,

$$-N_g \frac{d\alpha_g}{dt} = N_s \frac{d\alpha_s}{dt} + N_b \frac{d\alpha_b}{dt}, \quad [14]$$

where α_g is the fraction of ^{18}O in the gas phase, α_s is the fraction on the metal and on the ceria surface, and α_b is the fraction in the ceria bulk. N_g, N_s, and N_b are the total numbers of O atoms in the gas, on the catalyst surface, and in the bulk [earlier experiments had shown that practically all oxygen lattice atoms in ceria are exchangeable at 600°C (23)], respectively. α_s in each time step was obtained by integrating the above equation.

In addition, oxygen was allowed to dissociatively adsorb and desorb on Pt according to

$$O_{2(g)} + 2Pt \underset{r_{des}}{\overset{r_{ads}}{\rightleftarrows}} 2Pt\text{–}O. \quad [15]$$

For $^{16}O_2$, the adsorption rate is written

$$r_{ads,{}^{16}O_2} = k_{ads} p_{{}^{16}O_2}\left(1 - \theta_{{}^{16}O,Pt} - \theta_{{}^{18}O,Pt}\right)^2, \quad [16]$$

[2] In a following section, the bulk diffusion coefficient in ceria is estimated; see Eq. [24]. At 400°C, it has the value 3×10^{-23} m^2/s, which gives an even longer diffusion time: 320 h.

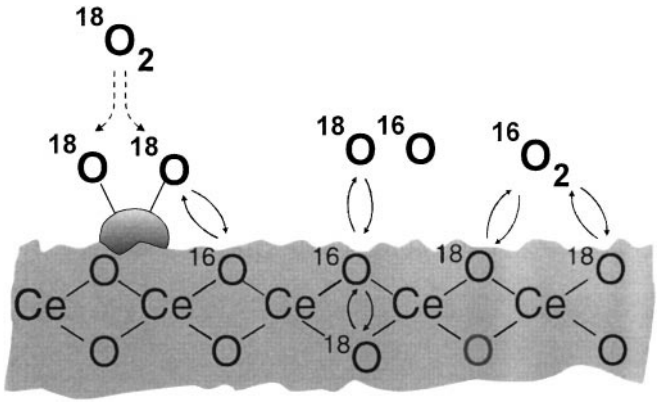

FIG. 4. Mechanisms of oxygen exchange on Pt/ceria.

and the desorption rate,

$$r_{\mathrm{des},^{16}\mathrm{O}_2} = k_{\mathrm{des}}\theta^2_{^{16}\mathrm{O,Pt}}. \quad [17]$$

The adsorption and desorption rates for $^{18}O_2$ and $^{16}O^{18}O$ are written analogously. In some simulations, the oxygen isotope compositions on Pt and in the ceria surface were allowed to be different (see point 2c above). A spillover oxygen exchange across the Pt perimeter between oxygen on Pt and on ceria was then allowed, according to

$$\mathrm{Pt}\text{–}^{18}\mathrm{O} + {}^{16}\mathrm{O}_{(s)} \underset{r_{-3}}{\overset{r_3}{\rightleftarrows}} \mathrm{Pt}\text{–}^{16}\mathrm{O} + {}^{18}\mathrm{O}_{(s)}, \quad [18]$$

with the rates

$$r_3 = k_{\mathrm{exch.spillover}}\theta_{^{18}\mathrm{O,Pt}}\theta_{^{16}\mathrm{O}}, \quad [19]$$

$$r_{-3} = k_{\mathrm{exch.spillover}}\theta_{^{16}\mathrm{O,Pt}}\theta_{^{18}\mathrm{O}}. \quad [20]$$

This rate expression should be considered formal, since the real exchange mechanism is likely more complicated. All the above presented exchange mechanisms, both direct on ceria and via Pt, are schematically illustrated in Fig. 4.

The temperature dependence of the rate coefficients for ceria was given according to Arrhenius expressions. For some of the parameters, a centered expression,

$$k_i^* = A_i^* \cdot \exp\left(-\frac{E_i}{R}\cdot\left(\frac{1}{T}-\frac{1}{T_{\mathrm{m}}}\right)\right), \quad [21]$$

was used to facilitate the regression. The reference temperature T_{m} was chosen to be 573 K.

Modeling Procedure

To obtain physically reasonable parameters for the adsorption and desorption of oxygen on Pt, the entropy change of oxygen adsorption at equilibrium, ΔS_{ads}, was set to 150 J/(mol, K). This value, although arbitrarily chosen, is reasonable because the entropy of oxygen in the gas phase is approximately 200 J/(mol, K) (30), and that the assumption of a two-dimensional gas gives $\Delta S_{\mathrm{ads}} = 100$ J/(mol, K), whereas localized adsorption gives $\Delta S_{\mathrm{ads}} = 180$ J/(mol, K) (31). The impact on the parameter values of the choice of ΔS_{ads} is quite small. For instance, if ΔS_{ads} is increased to 170 J/(mol, K), E_{des} will have to decrease about 10 kJ/mol to obtain the same value of the equilibrium constant. A_{des} was a free parameter in the model, whereas A_{ads} was calculated from the definitions of the equilibrium constant of adsorption and desorption (32),

$$A_{\mathrm{ads}} = A_{\mathrm{des}}\frac{1}{P_{\mathrm{r}}}\exp\left(\frac{\Delta S_{\mathrm{ads}}}{R}\right), \quad [22]$$

where $P_{\mathrm{r}} = 101325$ Pa. The energy of desorption, E_{des}, was set to a fraction of the energy of desorption for oxygen on Pt at low coverages, $E^0_{\mathrm{des}} = 240$ kJ/mol (10),

$$E_{\mathrm{des}} = E^0_{\mathrm{des}}(1 - a\theta_{\mathrm{O,Pt}}), \quad [23]$$

where $\theta_{\mathrm{O,Pt}}$ is the fractional coverage of oxygen on Pt and a is a parameter in the model. In this way, the lower desorption energy at high oxygen fractions (33) due to repulsive adsorbate–adsorbate interactions was taken into account. Finally, due to the large difference in activity for oxygen exchange between the low- and high-Pt-dispersion samples, the parameters governing the adsorption and desorption of oxygen on Pt were allowed to be different for these two samples.

Simulation Results

In Fig. 2 the results of the simulations with the above assumptions are shown. Generally, the simulations are in fairly good agreement with the experiments, especially when considering that the model is quite simple. The parameter values and their 95% individual confidence intervals are given in Table 2. The correlations between the parameters were, with a few exceptions, quite low. The preexponential factor of each rate constant is, as expected, strongly correlated to its activation energy (or, for the oxygen desorption, with its factor a). All other correlations were below ± 0.5.

From the parameter values in Table 2 it is seen that the lower activity of oxygen exchange for the HD sample is not, as one might expect, handled by higher activation energy for oxygen desorption from Pt. The activation energy is in fact lower (higher value of the parameter a) for this sample. Instead, the lower activity is explained by a lower frequency factor for desorption (A_{des}). The value is unusually low; given in the unit s^{-1} it corresponds to $\nu_{\mathrm{des}} = 2.2 \times 10^8$ s^{-1}, which is below the proposed interval for associative desorption of 10^{11}–10^{19} s^{-1} (34). These results may be explained when considering that a variation in oxygen adsorption and reactivity with the metal crystallite size has been observed for Pt supported on alumina (35). A limit in the Pt particle diameter of about 5 nm was observed. Pt particles

TABLE 2

Parameter Values from the Simulations of the Oxygen Exchange on Ceria and Pt/Ceria

Parameter	Value	95% Confidence interval	Unit
$A^*_{\text{exch.single}}$	2.6×10^{-15}	$\pm 0.3 \times 10^{-15}$	mol/(s, m^2 ceria, Pa)
$E_{\text{exch.single}}$	110	± 2	kJ/mol
$A^*_{\text{exch.multi.}}$	1.2×10^{-16}	$\pm 0.2 \times 10^{-16}$	mol/(s, m^2 ceria, Pa)
$E_{\text{exch.multi.}}$	175	± 3	kJ/mol
$A^*_{\text{bulk,diffusion}}$	5.1×10^{-24}	$\pm 0.2 \times 10^{-24}$	m^2/s
$E_{\text{bulk,diffusion}}$	55	± 0.8	kJ/mol
$E_{O_2\text{ ads HD}}$	0.91	± 0.04	kJ/mol
a_{HD}	0.587	± 0.052	—
$A_{\text{des HD}}$	4.4×10^3	$\pm 0.2 \times 10^3$	mol/(s, m^2 Pt)
$E_{O_2\text{ ads LD}}$	21	± 0.3	kJ/mol
a_{LD}	0.458	± 0.002	—
$A_{\text{des LD}}$	2.1×10^7	$\pm 0.08 \times 10^7$	mol/(s, m^2 Pt)

larger than 5 nm could be oxidized only in the surface layer, whereas Pt particles smaller than 5 nm underwent complete oxidation. Other studies have found that alumina-supported Pt particles smaller than 2 nm adsorb oxygen stronger (36, 37), tentatively either through subsurface oxidation or through a decreased effect of repulsive interactions between adsorbed oxygen atoms (37). Although Pt is normally not found capable of forming bulk oxides, it has been established that small metal particles (<2 nm) are different from bulk metal due to altered electronic properties (38). In our investigation, the average Pt particle sizes were 4.5 and 295 nm for the HD and LD samples, respectively. However, the particle size distribution was quite broad, with observed particle sizes for the HD sample ranging from 2 to 24 nm (particles smaller than 2 nm were difficult to observe). If the HD sample contains subsurface oxygen, the oxygen may have to pass through several atomic layers of oxygen when desorbing, which causes the frequencies of desorption to decrease. Such a decrease in the frequency factor may occur when there is a precursor step, although the effect on the Arrhenius parameters for desorption is expected to be weak (39). An alternative explanation to the low exchange activity of the HD sample is that reduction at 400°C induces some kind of strong metal–support interaction (SMSI). A SMSI had earlier been observed for PM/ceria as suppressed adsorption capacity of the metal, although normally after reduction temperatures above 500°C (18, 40, 41). However, oxidation at 300°C has been found sufficient to restore Pt/ceria after high-temperature reduction (41). In our investigation, most differences between the high- and low-dispersion samples were observed above 300°C, so a SMSI state does not seem likely.

The parameters for oxygen diffusion correspond to a diffusion coefficient of

$$D = 5.8 \times 10^{-19} \cdot \exp\left(-\frac{55 \times 10^3}{R \cdot T}\right) \quad \text{m}^2/\text{s}. \qquad [24]$$

The above expression was developed from data in the temperature range 25–600°C, but since there was little exchange below 400°C, it may be considered valid only in the range 400–600°C. The activation energy is somewhat lower than the value 89 kJ/mol, which was observed for polycrystalline CeO_2 in the temperature interval 850–1100°C (11). The predicted bulk diffusion coefficient at 350°C is about a factor of 40 lower than what had earlier been found for ceria (12). However, differences in ceria crystal structure may affect the results. Moreover, the methods for obtaining the diffusion coefficients were not the same. In the study by Martin and Duprez, the bulk diffusion coefficient was estimated from the slope of the fraction of ^{18}O in the gas phase after an initial period of about 100 s, which was considered long enough for the gas and the surface to equilibrate. Moreover, their experiments were conducted at a constant temperature of 350°C. It is likely that the concentration of oxygen vacancies is higher under these conditions compared with our study, in which the bulk diffusion coefficient was determined after a longer exposure to oxygen and at a higher temperature. These differences in experimental conditions may explain the large differences in the bulk diffusion coefficients.

CONCLUSIONS

The oxygen transport mechanisms in ceria, Pt/ceria, and Pt/alumina catalysts were investigated by isotope oxygen exchange. Exchange on ceria and Pt/ceria was modeled, and the rate-determining steps were found to be the adsorption/desorption of oxygen and bulk oxygen diffusion. Parameter values of these steps are presented. Both oxygen spillover and oxygen surface diffusion were found to be fast processes in comparison with the two processes mentioned above.

ACKNOWLEDGMENTS

Professor Bengt Kasemo is gratefully acknowledged for valuable discussions. The Swedish National Board for Industrial and Technological Development is acknowledged for financial support.

REFERENCES

1. Ghandi, H. S., Piken, A. G., Shelef, M., and Deloch, R. G., SAE Paper 760201, SAE Automotive Engineering Congress and Exposition, Detroit, MI, 1976.
2. Trovarelli, A., *Catal. Rev. Sci. Eng.* **38**, 439 (1996).
3. Ozawa, M., Kimura, M., and Isogai, A., *J. Alloys Compds.* **193**, 73 (1993).
4. Pijolat, M., Prin, M., Soustelle, M., Touret, O., and Nortier, P., *J. Chem. Soc. Faraday Trans.* **91**, 3941 (1995).
5. Fornasiero, P., Di Monte, R., Ranga Rao, G., Kaspar, J., Meriani, S., Trovarelli, A., and Graziani, M., *J. Catal.* **151**, 168 (1995).
6. Balducci, G., Kaspar, J., Fornasiero, P., Graziani, M., Islam, M. S., and Gale, J. D., *J. Phys. Chem. B* **101**, 1750 (1997).
7. Cho, B. K., *J. Catal.* **131**, 74 (1991).

8. Miki, T., Ogawa, T., Haneda, M., Kakuta, N., Ueno, A., Tateishi, S., Matsuura, S., and Sato, M., *J. Phys. Chem.* **94**, 6464 (1990).
9. Zhang, Y., Andersson, S., and Muhammed, M., *Appl. Catal. B* **6**, 325 (1995).
10. Boreskov, G. K., *in* "Catalysis—Science and Technology" (J. R. Anderson and M. Boudart, Eds.), Vol. 3, p. 43. Springer-Verlag, Berlin, 1982.
11. Steele, B. C. H., and Floyd, J. M., *Br. Ceram. Soc.* **19**, 55 (1971).
12. Martin, D., and Duprez, D., *J. Phys. Chem.* **100**, 9429 (1996).
13. Kramer, R., and Andre, M., *J. Catal.* **58**, 287 (1979).
14. Kakioka, H., Ducarme, V., and Teichner, S. J., *J. Chim. Phys.* **11/12**, 1715 (1971).
15. Klier, K., and Kucera, E., *J. Phys. Chem. Solids* **27**, 1087 (1966).
16. Katzer, J. R., Sleight, A. W., Gajardo, P., Michel, J. B., Gleason, E. F., and McMillan, S., *Disc. Faraday Soc.* **72**, 121 (1982).
17. Bernal, S., Calvino, J. J., Cifredo, G. A., Jobacho, A., Rodríguez-Izquierdo, J. M., Perrichon, V., and Laachir, A., *J. Catal.* **137**, 1 (1992).
18. Bernal, S., Botana, F. J., Calvino, J. J., Cauqui, M. A., Cifredo, G. A., Jobacho, A., Pintado, J. M., and Rodríguez-Izquierdo, J. M., *J. Phys. Chem.* **97**, 4118 (1993).
19. Duprez, D., and Madier, Y., personal communication, 1998.
20. Holmgren, A., unpublished experimental results, 1997.
21. Abderrahim, H., and Duprez, D., *in* "Catalysis and Automotive Pollution Control" (A. Crucq and A. Frennet, Eds.), Studies in Surface Science and Catalysis, Vol. 30, p. 359. Elsevier, Amsterdam, 1987.
22. Martin, D., and Duprez, D., *J. Phys. Chem.* **101**, 4428 (1997).
23. Holmgren, A., and Andersson, B., *J. Catal.* **178**, 14 (1998).
24. Cunningham, J., Cullinane, D., Farrell, F., O'Driscoll, J. P., and Morris, M. A., *J. Mater. Chem.* **5**, 1027 (1995).
25. Laachir, A., Perrichon, V., Badri, A., Lamotte, J., Catherine, E., Lavalley, J. C., El Fallah, J., Hilaire, L., le Normand, F., Quéméré, E., Sauvion, G. N., and Touret, O., *J. Chem. Soc. Faraday Trans.* **87**, 1601 (1991).
26. Klier, K., Nováková, J., and Jíru, P., *J. Catal.* **2**, 479 (1963).
27. Winter, E. R. S., *J. Chem. Soc.* **1**, 2889 (1968).
28. Li, C., Domen, K., Maruya, K., and Onishi, T., *J. Am. Chem. Soc.* **111**, 7683 (1989).
29. Finlayson, B. A., "Nonlinear Analysis in Chemical Engineering." McGraw–Hill, New York, 1980.
30. Barin, I., "Thermochemical Data of Pure Substances." VCH, Weinheim, 1993.
31. Knox, D., and Dadyburjor, D. B., *Chem. Eng. Commun.* **11**, 99 (1981).
32. Masel, R. I., "Principles of Adsorption and Reaction on Solid Surfaces." Wiley, New York, 1996.
33. Campbell, C. T., Ertl, G., Kuipers, H., and Segner, J., *Surf. Sci.* **107**, 220 (1981).
34. Zhdanov, V. P., Pavlícek, J., and Knor, Z., *Catal. Rev. Sci. Eng.* **30**, 501 (1988).
35. Herz, R. K., and Shinouskis, E. J., *Appl. Surf. Sci.* **19**, 373 (1984).
36. Briot, P., Auroux, A., Jones, D., and Primet, M., *Appl. Catal.* **59**, 141 (1990).
37. Putna, E. S., Vohs, J. M., and Gorte, R. J., *Surf. Sci.* **391**, L1178 (1997).
38. van Broekhoven, E. H., and Ponec, V., *Surf. Sci.* **162**, 731 (1985).
39. Zhdanov, V. P., *Surf. Sci. Rep.* **12**, 183 (1991).
40. Daniel, D. W., *J. Phys. Chem.* **92**, 3891 (1988).
41. Golunski, S. E., Hatcher, H. A., Rajaram, R. R., and Truex, T. J., *Appl. Catal. B* **5**, 367 (1995).